Measurement of the Beam-Spin Azimuthal Asymmetry Associated with Deeply-Virtual Compton Scattering

A. Airapetian,[31] N. Akopov,[31] Z. Akopov,[31] M. Amarian,[26,31] E. C. Aschenauer,[7] H. Avakian,[11] R. Avakian,[31] A. Avetissian,[31] E. Avetissian,[31] P. Bailey,[15] B. Bains,[15] V. Baturin,[24] C. Baumgarten,[21] M. Beckmann,[12] S. Belostotski,[24] S. Bernreuther,[29] N. Bianchi,[11] H. Böttcher,[7] A. Borissov,[6,19] O. Bouhali,[23] M. Bouwhuis,[15] J. Brack,[5] S. Brauksiepe,[12] W. Brückner,[14] A. Brüll,[18] I. Brunn,[9] H. J. Bulten,[23,30] G. P. Capitani,[11] P. Chumney,[22] E. Cisbani,[26] G. Ciullo,[10] G. R. Court,[16] P. F. Dalpiaz,[10] R. De Leo,[3] L. De Nardo,[1] E. De Sanctis,[11] D. De Schepper,[2] E. Devitsin,[20] P. K. A. de Witt Huberts,[23] P. Di Nezza,[11] M. Düren,[9] M. Ehrenfried,[7] G. Elbakian,[31] F. Ellinghaus,[7] J. Ely,[5] R. Fabbri,[10] A. Fantoni,[11] A. Fechtchenko,[8] L. Felawka,[28] B. W. Filippone,[4] H. Fischer,[12] B. Fox,[5] J. Franz,[12] S. Frullani,[26] Y. Gärber,[7,9] F. Garibaldi,[26] E. Garutti,[23] G. Gavrilov,[24] V. Gharibyan,[31] A. Golendukhin,[6,21,31] G. Graw,[21] O. Grebeniouk,[24] P. W. Green,[1,28] L. G. Greeniaus,[1,28] A. Gute,[9] W. Haeberli,[17] K. Hafidi,[2] M. Hartig,[28] D. Hasch,[9,11] D. Heesbeen,[23] F. H. Heinsius,[12] M. Henoch,[9] R. Hertenberger,[21] W. H. A. Hesselink,[23,30] G. Hofman,[5] Y. Holler,[6] R. J. Holt,[15] B. Hommez,[13] G. Iarygin,[8] A. Izotov,[24] H. E. Jackson,[2] A. Jgoun,[24] P. Jung,[7] R. Kaiser,[7] J. Kanesaka,[29] E. Kinney,[5] A. Kisselev,[2,24] P. Kitching,[1] H. Kobayashi,[29] N. Koch,[9] K. Königsmann,[12] H. Kolster,[18,23] V. Korotkov,[7] E. Kotik,[1] V. Kozlov,[20] B. Krauss,[9] V. G. Krivokhijine,[8] G. Kyle,[22] L. Lagamba,[3] A. Laziev,[23,30] P. Lenisa,[10] P. Liebing,[7] T. Lindemann,[6] W. Lorenzon,[19] A. Maas,[7] N. C. R. Makins,[15] H. Marukyan,[31] F. Masoli,[10] M. McAndrew,[16] K. McIlhany,[4,18] F. Meissner,[9,21] F. Menden,[12] N. Meyners,[6] O. Mikloukho,[24] C. A. Miller,[1,28] R. Milner,[18] V. Muccifora,[11] R. Mussa,[10] A. Nagaitsev,[8] E. Nappi,[3] Y. Naryshkin,[24] A. Nass,[9] K. Negodaeva,[7] W.-D Nowak,[7] K. Oganessyan,[6,11] T. G. O'Neill,[2] B. R. Owen,[15] S. F. Pate,[22] S. Potashov,[20] D. H. Potterveld,[2] M. Raithel,[9] G. Rakness,[5] V. Rappoport,[24] R. Redwine,[18] D. Reggiani,[10] A. R. Reolon,[11] K. Rith,[9] D. Robinson,[15] A. Rostomyan,[31] M. Ruh,[12] D. Ryckbosch,[13] Y. Sakemi,[29] I. Sanjiev,[2,24] F. Sato,[29] I. Savin,[8] C. Scarlett,[19] A. Schäfer,[25] C. Schill,[12] F. Schmidt,[9] G. Schnell,[22] K. P. Schüler,[6] A. Schwind,[7] J. Seibert,[12] B. Seitz,[1] T.-A. Shibata,[29] V. Shutov,[8] M. C. Simani,[23,30] A. Simon,[12] K. Sinram,[6] E. Steffens,[9] J. J. M. Steijger,[23] J. Stewart,[2,16,28] U. Stösslein,[5] K. Suetsugu,[29] S. Taroian,[31] A. Terkulov,[20] S. Tessarin,[10] E. Thomas,[11] B. Tipton,[4] M. Tytgat,[13] G. M. Urciuoli,[26] J. F. J. van den Brand,[23,30] G. van Steenhoven,[23] R. van Vyver,[13] J. J. van Hunen,[23] M. C. Vetterli,[27,28] V. Vikhrov,[24] M. G. Vincter,[1] J. Visser,[23] C. Weiskopf,[9] J. Wendland,[27,28] J. Wilbert,[9] T. Wise,[17] S. Yen,[28] S. Yoneyama,[29] and H. Zohrabian[31]

(HERMES Collaboration)

[1]*Department of Physics, University of Alberta, Edmonton, Alberta T6G 2J1, Canada*
[2]*Physics Division, Argonne National Laboratory, Argonne, Illinois 60439-4843*
[3]*Istituto Nazionale di Fisica Nucleare, Sezione di Bari, 70124 Bari, Italy*
[4]*W. K. Kellogg Radiation Laboratory, California Institute of Technology, Pasadena, California 91125*
[5]*Nuclear Physics Laboratory, University of Colorado, Boulder, Colorado 80309-0446*
[6]*DESY, Deutsches Elektronen Synchrotron, 22603 Hamburg, Germany*
[7]*DESY Zeuthen, 15738 Zeuthen, Germany*
[8]*Joint Institute for Nuclear Research, 141980 Dubna, Russia*
[9]*Physikalisches Institut, Universität Erlangen-Nürnberg, 91058 Erlangen, Germany*
[10]*Istituto Nazionale di Fisica Nucleare, Sezione di Ferrara and Dipartimento di Fisica, Università di Ferrara, 44100 Ferrara, Italy*
[11]*Istituto Nazionale di Fisica Nucleare, Laboratori Nazionali di Frascati, 00044 Frascati, Italy*
[12]*Fakultät für Physik, Universität Freiburg, 79104 Freiburg, Germany*
[13]*Department of Subatomic and Radiation Physics, University of Gent, 9000 Gent, Belgium*
[14]*Max-Planck-Institut für Kernphysik, 69029 Heidelberg, Germany*
[15]*Department of Physics, University of Illinois, Urbana, Illinois 61801*
[16]*Physics Department, University of Liverpool, Liverpool L69 7ZE, United Kingdom*
[17]*Department of Physics, University of Wisconsin-Madison, Madison, Wisconsin 53706*
[18]*Laboratory for Nuclear Science, Massachusetts Institute of Technology, Cambridge, Massachusetts 02139*
[19]*Randall Laboratory of Physics, University of Michigan, Ann Arbor, Michigan 48109-1120*
[20]*Lebedev Physical Institute, 117924 Moscow, Russia*
[21]*Sektion Physik, Universität München, 85748 Garching, Germany*
[22]*Department of Physics, New Mexico State University, Las Cruces, New Mexico 88003*
[23]*Nationaal Instituut voor Kernfysica en Hoge-Energiefysica (NIKHEF), 1009 DB Amsterdam, The Netherlands*
[24]*Petersburg Nuclear Physics Institute, St. Petersburg, Gatchina, 188350 Russia*

 0031-9007/01/87(18)/182001(5)$15.00

[25]*Institut für Theoretische Physik, Universität Regensburg, 93040 Regensburg, Germany*
[26]*Istituto Nazionale di Fisica Nucleare, Sezione Roma 1, Gruppo Sanità and Physics Laboratory, Istituto Superiore di Sanità, 00161 Roma, Italy*
[27]*Department of Physics, Simon Fraser University, Burnaby, British Columbia V5A 1S6, Canada*
[28]*TRIUMF, Vancouver, British Columbia V6T 2A3, Canada*
[29]*Department of Physics, Tokyo Institute of Technology, Tokyo 152, Japan*
[30]*Department of Physics and Astronomy, Vrije Universiteit, 1081 HV Amsterdam, The Netherlands*
[31]*Yerevan Physics Institute, 375036 Yerevan, Armenia*
(Received 18 June 2001; published 10 October 2001)

The beam-spin asymmetry in hard electroproduction of photons has been measured. The data have been accumulated by the HERMES experiment at DESY using the HERA 27.6 GeV longitudinally polarized positron beam and an unpolarized hydrogen-gas target. The asymmetry in the azimuthal distribution of the produced photons in the angle ϕ relative to the lepton scattering plane was determined with respect to the helicity state of the incoming positron beam. The beam-spin analyzing power in the $\sin\phi$ moment was measured to be $-0.23 \pm 0.04(\text{stat}) \pm 0.03(\text{syst})$ in the missing-mass range below 1.7 GeV. The observed asymmetry is attributed to the interference of the Bethe-Heitler and deeply virtual Compton scattering processes.

DOI: 10.1103/PhysRevLett.87.182001 PACS numbers: 13.60.Fz, 14.20.Dh, 24.85.+p

The internal structure of the nucleon has been extensively studied in deep-inelastic lepton scattering, resulting in such measurements as the momentum distributions of quarks and their helicity dependences. The contribution of the quark spins to the nucleon spin was found to be small. Recently a possibility was identified to study experimentally the total contributions of partons to the nucleon spin, including their orbital angular momenta [1]. This idea is based on the formalism of the so-called skewed parton distributions (SPD) (also referred to as off-forward or generalized parton distributions in the literature [2–5]). In this formalism dynamical correlations between partons with different momenta are taken into account. The SPD framework embodies a wide range of observables, such as electromagnetic form factors, conventional parton distributions, and hard exclusive cross sections. In particular, sum rules [5–7] relate second moments of certain SPDs with the total angular momenta of the quarks and of the gluons in the nucleon.

A reaction that can be cleanly interpreted in terms of SPDs is deeply virtual Compton scattering (DVCS), i.e., the exclusive leptoproduction of a single multi-GeV photon with the target nucleon remaining intact. Unfortunately, experimental information on DVCS is scant. A central issue is that it is impossible to distinguish between photons originating from DVCS and those from the Bethe-Heitler (BH) process, which can be much more copious. The corresponding diagrams are shown in Fig. 1. However, the interference between the DVCS and BH processes can be exploited in order to obtain information on DVCS amplitudes. For that purpose HERMES Collaboration has measured the beam-spin asymmetry in hard exclusive electroproduction of photons. The data obtained are presented in this paper.

Using the notation of Ref. [8], the cross section for exclusive leptoproduction of photons can be written as

$$\frac{d^4\sigma}{d\phi\, dt dQ^2 dx} = \frac{xy^2}{32(2\pi)^4 Q^4} \frac{|\tau_{\text{BH}} + \tau_{\text{DVCS}}|^2}{(1 + 4x^2m^2/Q^2)^{1/2}}, \quad (1)$$

where x represents the Bjorken scaling variable, $y = \nu/E$ the fraction of the incident lepton energy E carried by the virtual photon, with ν its energy and $-Q^2$ its four momentum squared, m is the proton mass, and τ_{BH} and τ_{DVCS} are the BH and DVCS amplitudes. The cross section shown is a differential in x, Q^2, ϕ, and t, where the azimuthal angle ϕ is the angle between the lepton scattering plane and the plane defined by the virtual and real photons, and t represents the square of the four-momentum transfer to the target.

In Ref. [8] expressions are given for the DVCS + BH cross sections in leading order $\mathcal{O}(1/Q)$. (An alternative approach can be found in Ref. [9], for instance.) The leading-order interference term that depends on the helicity of the incident lepton is

$$(\tau^*_{\text{BH}}\tau_{\text{DVCS}} + \tau^*_{\text{DVCS}}\tau_{\text{BH}})_{\text{pol}} = \frac{4\sqrt{2}\,me^6}{tQx} \frac{1}{\sqrt{1-x}} e_l P_l \left[-\sin\phi \sqrt{\frac{1+\epsilon}{\epsilon}}\, \text{Im}\tilde{M}^{1,1} \right]. \quad (2)$$

The quantity $\tilde{M}^{1,1}$ is the linear combination of DVCS helicity amplitudes that contributes to the case of a polarized beam and an unpolarized target. The interference is seen to depend on the azimuthal angle ϕ, the sign of the lepton charge e_l, and the polarization P_l of the incident lepton. The kinematic quantity ϵ is the polarization parameter of the virtual photon. A determination of the $\sin\phi$ moment of the asymmetry of the interference term shown in Eq. (2) with respect to the beam polarization provides information on the imaginary part of the DVCS amplitude combination $\tilde{M}^{1,1}$, which is related to the SPDs [8]. Not shown in Eq. (2) are other interference terms that are suppressed by $\mathcal{O}(1/Q)$, but they involve other ϕ moments.

The data presented here were recorded during the 1996 and 1997 running periods of the HERMES experiment

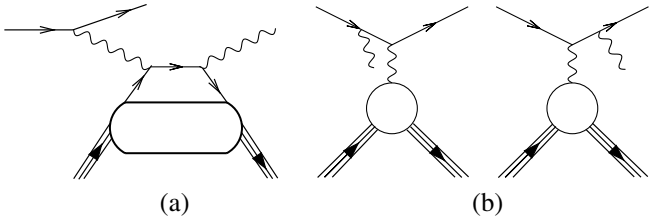

FIG. 1. (a) Feynman diagram for deeply virtual Compton scattering and (b) photon radiation from the incident and scattered leptons in the Bethe-Heitler process.

using the 27.6-GeV HERA longitudinally polarized positron beam at DESY [10]. The beam polarization was continuously measured by Compton backscattering and had an average value of 0.55 with a fractional uncertainty of 3.8% [11,12]. The positrons were scattered off a hydrogen-gas target [13]. Both unpolarized and spin-averaged polarized-target data have been used in the analysis.

The scattered positrons and coincident photons were detected by the HERMES spectrometer [14] in the polar-angle range of 40–220 mrad. A positron trigger was formed from a coincidence between three scintillator hodoscope planes and a lead-glass calorimeter. The trigger required an energy of more than 3.5 GeV deposited in the calorimeter. Charged particle identification was based on information from four detectors: a threshold Čerenkov counter, a transition radiation detector, a preshower scintillator counter, and a lead-glass calorimeter. The particle identification provides an average positron identification efficiency of 99% with a hadron contamination of less than 1%. Photons are identified by the detection of energy deposition in the calorimeter and the preshower counter without an associated charged track.

Events were selected if they contained only one positron track with momentum larger than 3.5 GeV and only one photon with an energy deposition greater than 0.8 GeV in the calorimeter. The following requirements were imposed on the positron kinematics: $Q^2 > 1\ \mathrm{GeV}^2$, $W^2 > 4\ \mathrm{GeV}^2$, and $\nu < 24$ GeV, where W denotes the photon-nucleon invariant mass.

In Fig. 2, the missing-mass distribution of the selected events is compared to the results of a Monte Carlo (MC) simulation in which photons from fragmentation processes in deep-inelastic scattering (DIS) and from the exclusive BH process, $e + p \rightarrow e' + \gamma + p$, are included. The missing mass is defined as $M_x^2 = (q + P_p - k)^2$ with q, P_p, and k being the four momenta of the virtual photon, the target nucleon, and the produced real photon, respectively. Because of the finite-momentum resolution of the spectrometer, M_x^2 may be negative, in which case we define $M_x = -\sqrt{-M_x^2}$.

The MC calculation is normalized to the same number of deep inelastically scattered positrons as were observed inclusively in the experiment (about 5.1 million DIS events), which corresponds to an integrated luminosity of 104 pb^{-1}. There is fairly good agreement between the data and the MC results in the relevant kinematic range of the photon spectrum. In the region of low missing mass, the main contribution is due to the BH process, while the smeared DIS contribution is almost negligible. The smearing of the data to negative M_x^2 values is well reproduced by the Monte Carlo calculation, which does not include the DVCS process. This result is consistent with the calculations of Ref. [15], where it is shown that the DVCS contribution to the electroproduction of photons is less than 10% for the present kinematics.

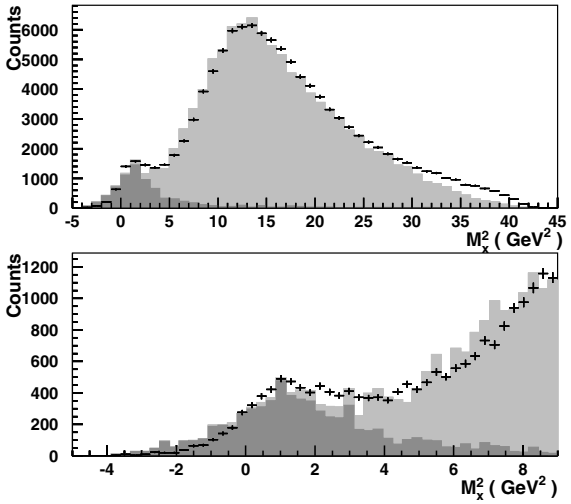

FIG. 2. The measured distribution of photons observed in hard electroproduction versus the missing mass squared M_x^2. In the upper panel the full kinematic range is displayed, while the low M_x^2 domain is shown in the lower panel. The light-gray histogram represents the results of a Monte Carlo simulation in which fragmentation processes and the Bethe-Heitler process are included, while the dark-shaded histogram represents only the BH contribution. The Monte Carlo simulation includes the effect of the detector resolution.

Photon pairs from the π^0 decay are removed from the data by requiring the presence of exactly one photon cluster in the (segmented) calorimeter. There could be a remaining π^0 contamination from photon pairs that cannot be spatially resolved by the granularity of the calorimeter. It may also happen that one of the π^0 decay photons escapes detection. These contaminations have been estimated in the nominal exclusive region using a Monte Carlo simulation. It was found that π^0 mesons produced in exclusive processes or as fragmentation products in deep-inelastic scattering may contaminate the exclusive part of the photon spectrum by at most 8.5%.

The DVCS-BH interference terms can be extracted from the dependence of the data on the azimuthal angle ϕ. In order to have an almost full ϕ coverage, events were selected with $15 < \theta_{\gamma\gamma^*} < 70$ mrad, where $\theta_{\gamma\gamma^*}$ represents the angle between the directions of the virtual photon and the real photon. A MC simulation shows that, for angles smaller than 15 mrad, the granularity of the calorimeter ($9 \times 9\ \mathrm{cm}^2$) is insufficient to reliably determine the angle

ϕ. For angles larger than 70 mrad, the ϕ acceptance is restricted. The average ϕ resolution in the selected $\theta_{\gamma\gamma^*}$ range is about 0.14 rad.

In Fig. 3, the azimuthal dependence of the measured beam-spin asymmetry A_{LU} is shown, which is defined as

$$A_{LU}(\phi) = \frac{1}{\langle |P_l| \rangle} \frac{N^+(\phi) - N^-(\phi)}{N^+(\phi) + N^-(\phi)}, \qquad (3)$$

where N^+ and N^- represent the luminosity-normalized yields of events with corresponding beam helicity states, $\langle |P_l| \rangle$ is the average magnitude of the beam polarization, and the subscripts L and U denote a longitudinally polarized beam and an unpolarized target. The data displayed in Fig. 3 were selected requiring a missing mass between -1.5 and $+1.7$ GeV, i.e., -3σ below and $+1\sigma$ above $M_x = m$, and represent 4015 events. An asymmetric M_x range was chosen to minimize the influence of the DIS-fragmentation background while optimizing the statistics. Both the proton and the $\Delta(1232)$ resonance are included in the selected M_x range. However, the data most likely originate from the exclusive final state with one proton, since the scattering process is dominated by the elastic contribution at kinematics relevant for the BH process. This conclusion is supported experimentally by Fig. 2, where the elastic BH Monte Carlo gives a good account of the photon spectrum at low M_x, and theoretically in Ref. [16]. The comparison of the A_{LU} data in Fig. 3 to a simple $\sin\phi$ curve demonstrates that the data have the ϕ dependence expected from Eq. (2). The model calculation of Ref. [17] which is based on the SPD framework and computed at the average kinematics of the present experiment has also been displayed.

In order to be able to compare the ϕ dependence of the beam-spin asymmetry for various missing-mass bins, the $\sin\phi$ weighted moments have been determined:

$$A_{LU}^{\sin\phi^\pm} = \frac{2}{N^\pm} \sum_{i=1}^{N^\pm} \frac{\sin\phi_i}{|P_l|_i}, \qquad (4)$$

where the superscript $\pm$ refers to the helicity of the positron beam. In Fig. 4 the extracted values of $A_{LU}^{\sin\phi^\pm}$ are plotted versus the missing mass M_x for the two helicity states λ_{beam} of the positron beam. The sign of the $\sin\phi$ moment is opposite for the two beam helicities, in agreement with the expectations for the helicity dependence of the relevant DVCS-BH interference term. The beam-spin averaged data are consistent with zero, which is in agreement with the expectations for an unpolarized beam and target. The beam-spin averaged data can be used to determine an upper limit of a possible false asymmetry due to instrumental effects which—averaged for M_x between -1.5 and $+1.7$ GeV—amounts to -0.03 ± 0.04.

Since the data in Fig. 4 for the two beam helicity states contain the same physics information, they are combined when evaluating the beam-spin analyzing power $A_{LU}^{\sin\phi}$:

$$A_{LU}^{\sin\phi} = \frac{2}{N} \sum_{i=1}^{N} \frac{\sin\phi_i}{(P_l)_i}, \qquad (5)$$

where $N = N^+ + N^-$. In contrast to Eq. (4), the sign of the beam polarization is explicitly taken into account, thus distinguishing the two helicity states. The results are presented in Fig. 5 versus missing-mass. All bins in the missing-mass region below $M_x \approx 2.5$ GeV show a similar negative asymmetry, while $A_{LU}^{\sin\phi}$ is consistent with zero for

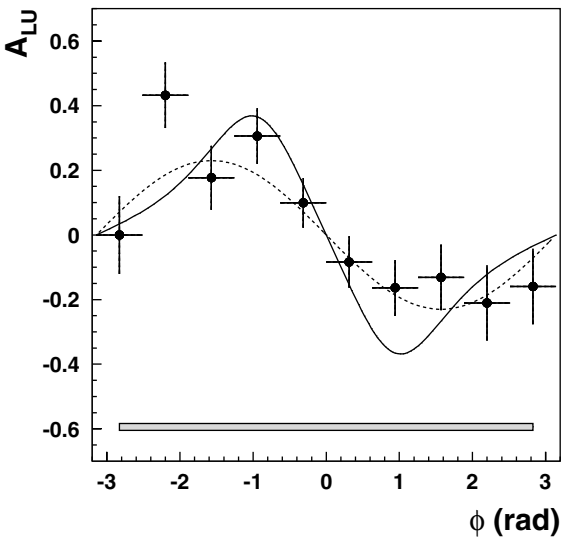

FIG. 3. Beam-spin asymmetry A_{LU} for hard electroproduction of photons as a function of the azimuthal angle ϕ. The data correspond to the missing-mass region between -1.5 and $+1.7$ GeV. The dashed curve represents a $\sin\phi$ dependence with an amplitude of 0.23, while the solid curve represents the result of a model calculation taken from Ref. [17]. The horizontal error bars represent the bin width, and the error band below represents the systematic uncertainty.

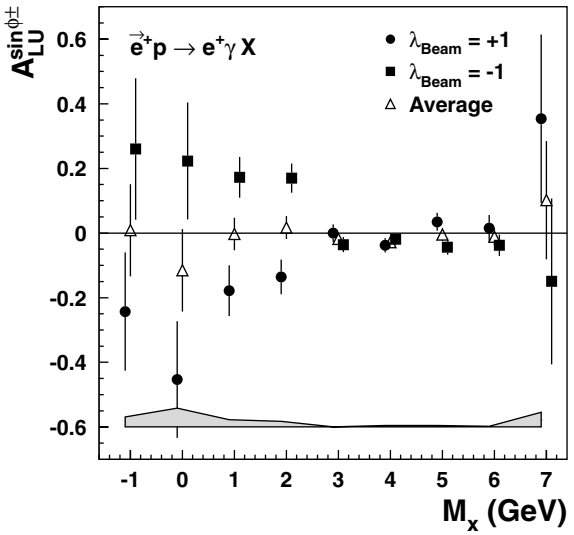

FIG. 4. The $\sin\phi$ moment $A_{LU}^{\sin\phi^\pm}$ as a function of the missing mass for positive beam helicity (circles), negative beam helicity (squares), and the averaged helicity (open triangles). A negative value is assigned to M_x if $M_x^2 < 0$. The error bars are statistical only. The systematic uncertainty is represented by the error band at the bottom of the figure.

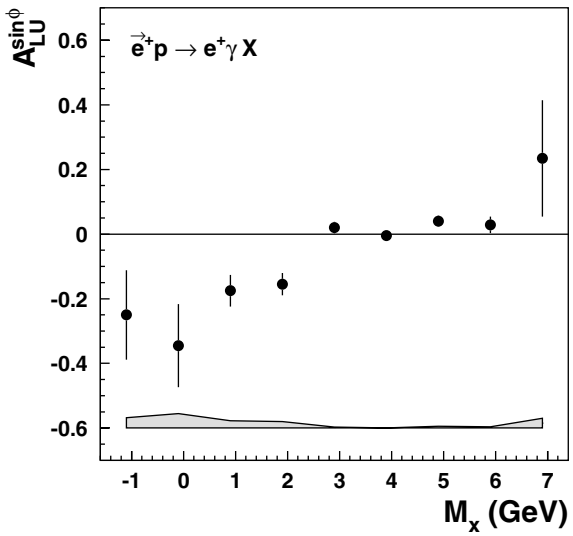

FIG. 5. The beam-spin analyzing power $A_{LU}^{\sin\phi}$ for hard electroproduction of photons on hydrogen as a function of the missing mass. The systematic uncertainty is represented by the error band at the bottom of the figure.

larger M_x values. Consequently smeared DIS events at low M_x can only marginally dilute the observed asymmetry. As the missing-mass resolution of the HERMES spectrometer for DVCS-like events is $\sim$0.77 GeV, part of the exclusive data falls below or above m. As a result the missing-mass bins left and right of $M_x = m$ also show a nonzero value of $A_{LU}^{\sin\phi}$ in Fig. 5.

In order to evaluate the systematic uncertainty on $A_{LU}^{\sin\phi}$ several contributions were considered. The same MC simulation described above was used to estimate the smearing effect on $A_{LU}^{\sin\phi}$, which was found to be less than 5%. The systematic uncertainty associated with smearing and beam polarization is represented by the error bands displayed in Figs. 3–5. In the exclusive region ($-1.5 < M_x < 1.7$ GeV), two additional contributions to the systematic uncertainty were considered. Possible false asymmetries due to the BH process are at most 2.6%, while the uncertainty due to the π^0 contamination is estimated to be 12.5%. The total systematic uncertainty at $M_x \approx m$ amounts to 0.03. The quoted instrumental false asymmetry has not been included in this number as it cancels in $A_{LU}^{\sin\phi}$.

By combining the $A_{LU}^{\sin\phi}$ data in the same M_x region as was used for Fig. 3 ($-1.5 < M_x < 1.7$ GeV), an average value of $-0.23 \pm 0.04(\text{stat}) \pm 0.03(\text{syst})$ is obtained. The average values of the kinematic variables corresponding to this measurement are $\langle x \rangle = 0.11$, $\langle Q^2 \rangle = 2.6$ GeV^2, and $\langle -t \rangle = 0.27$ GeV^2. Since the BH process is dominated by the exclusive final state with one proton [16], and interference can only occur between processes with identical final states, the measured beam-spin analyzing power can be compared to calculations for exclusive processes which are based on the SPD framework. In Ref. [17], e.g., a value of -0.37 is quoted for $A_{LU}^{\sin\phi}$ in a calculation for kinematics close to those of the present experiment. This calculation includes a twist-3 contribution of less than 5%.

In summary, the beam-spin azimuthal asymmetry for hard electroproduction of photons has been measured in the missing-mass (M_x) range up to 7 GeV. A nonzero asymmetry is observed in the exclusive domain, i.e., for $M_x \leq 1.7$ GeV. The observed $\sin\phi$ moment of the data has the beam helicity dependence expected from interference between deeply virtual Compton scattering and the Bethe-Heitler process.

We gratefully acknowledge the DESY management for its support, the staffs at DESY and the collaborating institutions for their significant effort, and our funding agencies for financial support.

[1] X. Ji, Phys. Rev. Lett. **78**, 610 (1997).
[2] F. M. Dittes, D. M. Müller, D. Robaschik, B. Geyer, and J. Horejsi, Phys. Lett. B **209**, 325 (1988).
[3] D. Müller *et al.,* Fortschr. Phys. **42**, 101 (1994).
[4] A. V. Radyushkin, Phys. Lett. B **385**, 333 (1996).
[5] X. Ji, Phys. Rev. D **55**, 7114 (1997).
[6] B. W. Filippone and X. Ji, Adv. Nucl. Phys. (to be published), hep-ph/0101224.
[7] R. L. Jaffe, Nucl. Phys. **B536**, 303 (1998).
[8] M. Diehl *et al.,* Phys. Lett. B **411**, 193 (1997).
[9] A. V. Belitsky *et al.,* Nucl. Phys. B **593**, 289 (2001).
[10] D. P. Barber *et al.,* Phys. Lett. B **343**, 436 (1995).
[11] HERMES Collaboration, A. Airapetian *et al.,* Phys. Lett. B **442**, 484 (1998).
[12] M. Beckmann *et al.,* Nucl. Instrum. Methods (to be published), physics/0009047.
[13] J. Stewart, in *Polarized Gas Targets and Polarized Beams,* edited by R. J. Holt and M. A. Miller, AIP Conf. Proc. No. 421 (AIP, New York, 1998), p. 69.
[14] HERMES Collaboration, K. Ackerstaff *et al.,* Nucl. Instrum. Methods Phys. Res., Sect. A **417**, 230 (1998).
[15] P. A. M. Guichon and M. Vanderhaeghen, Prog. Part. Nucl. Phys. **41**, 125 (1998); M. Vanderhaeghen, P. A. M. Guichon, and M. Guidal, Phys. Rev. Lett. **80**, 5064 (1998).
[16] L. L. Frankfurt, M. V. Polyakov, and M. Strikman, hep-ph/9808449.
[17] N. Kivel, M. Polyakov, and M. Vanderhaeghen, Phys. Rev. D **63**, 114014 (2001).